Biological and Medical Applications of Materials and Interfaces

Comb-Like Pseudopeptides Enable Very Rapid and Efficient Intracellular Trehalose Delivery for Enhanced Cryopreservation of Erythrocytes

Siyuan Chen, Liwei Wu, Jie Ren, Victoria L. Bemmer, Richard Zajicek, and Rongjun Chen

Just Accepted

Comb-Like Pseudopeptides Enable Very Rapid and Efficient Intracellular Trehalose Delivery for Enhanced Cryopreservation of Erythrocytes

Siyuan Chen [a‡], Liwei Wu [a‡], Jie Ren [a], Victoria Bemmer [b], Richard Zajicek [c], Rongjun Chen [a]*

[a.] Department of Chemical Engineering, Imperial College London, South Kensington Campus, London, SW7 2AZ, United Kingdom

[b.] Department of Materials, Imperial College London, South Kensington Campus, London, SW7 2AZ, United Kingdom

[c.] Cell & Gene Therapy Platform CMC, Platform Technology & Sciences, GlaxoSmithKline plc R&D, Gunnels Wood, Stevenage, Hertfordshire SG1 2NY, United Kingdom

*Corresponding author: rongjun.chen@imperial.ac.uk

[‡] Equal contribution to this study.

KEYWORDS: pH-responsive; pseudopeptide; comb-like polymer; cryopreservation; blood; trehalose

ABSTRACT

Cell cryopreservation plays a key role in development of reproducible and cost-effective cell-based therapies. Trehalose accumulated in freezing and desiccation tolerant organisms in nature has been sought as an attractive non-toxic cryoprotectant. Herein, we report a co-incubation method for very rapid and efficient delivery of membrane-impermeable trehalose into ovine erythrocytes through reversible membrane permeabilization using pH-responsive, comb-like pseudopeptides. The pseudopeptidic polymers containing relatively long alkyl side chains were synthesized to mimic membrane-anchoring fusogenic proteins. The intracellular trehalose delivery efficiency was optimized by manipulating the side chain length, degree of substitution and concentration of the pseudopeptides with different hydrophobic alkyl side chains, the pH, temperature and time of incubation, as well as the polymer-to-cell ratio and the concentration of extracellular trehalose. Treatment of erythrocytes with the comb-like pseudopeptides for only 15 min yielded an intracellular trehalose concentration of 177.9 ± 8.6 mM, which resulted in $90.3 \pm 0.7\%$ survival after freeze-thaw. The very rapid and efficient delivery was found to be attributed to the reversible, pronounced membrane curvature change as a result of strong membrane insertion of the comb-like pseudopeptides. The pseudopeptides can enable efficient intracellular delivery of not only trehalose for improved cell cryopreservation, but also other membrane-impermeable cargos.

1. Introduction

It remains a major challenge to delivering hydrophilic, membrane-impermeable molecules into the cell interior.[1] Clinical applications of polar biomolecules, such as nucleic acids, recombinant therapeutic proteins, enzymes, monoclonal antibodies and saccharides, can be impaired by inefficient intracellular delivery.[2–5] Therefore, there is an urgent need to develop delivery vehicles, which may facilitate efficient intracellular delivery of hydrophilic, membrane-impermeable molecules to their target sites without causing cytotoxicity.[6]

Cryopreservation of therapeutic cells is crucial for the development of reproducible and cost-effective cell-based therapies. Conventional cryoprotectants such as dimethyl sulfoxide (DMSO) and glycerol are commonly used for cell cryopreservation.[7] In order to ensure a steady blood supply especially for rare blood groups, erythrocytes are usually cryopreserved with glycerol to prolong its shelf-life.[8,9] However, deglycerolization must be performed after thawing to avoid post-transfusion osmotic haemolysis, which is not only labor-intensive and technically demanding, but also results in considerably reduced cell viability by 15-20%.[10,11] Therefore, there is increasing interest in developing an alternative method for improved erythrocyte cryopreservation. Trehalose, a hydrophilic non-reducing disaccharide of glucose, accumulates in a range of freezing and desiccation tolerant organisms in nature and has attracted tremendous attention in the field of cell preservation.[12–14]

Trehalose is required to be present both inside and outside a cell to ensure optimum bioprotection during preservation.[15] Unfortunately, mammalian cells are incapable of synthesizing or importing trehalose.[14] Efficient intracellular delivery of trehalose is challenging due to its membrane-impermeable and hydrophilic nature. Several approaches have been investigated to achieve intracellular trehalose localization, including physical methods such as microinjection[16]

and electroporation[17], biological methods such as mutant bacterial toxins[18] and intracellular trehalose synthesis through genetic engineering[19], and chemical methods such as liposomes[20]. However, these methods are limited due to either lack of scalability (e.g. microinjection), or insufficient intracellular trehalose for desired bioprotection (e.g. liposomes)[21]. Besides, some invasive approaches (e.g. electroporation, mutant bacterial toxins) may affect membrane integrity and have safety concerns.[22]

This study employs amphiphilic synthetic biopolymers to enhance membrane permeability in order to improve intracellular trehalose delivery without causing obvious cell damage. A class of biodegradable, pH-responsive pseudopeptides has been recently developed to mimic the pH-responsive, membrane-permeabilizing activity of fusogenic viral peptides. The biomimetic pseudopeptidic polymers have been synthesized by grafting hydrophobic natural amino acids, such as L-phenylalanine, onto the pendant carboxylic acid groups of an anionic, metabolite-derived polyamide, poly(L-lysine isophthalamide) (PLP).[23-25] Unlike pathogenic viruses or viral peptides which have safety concerns and production difficulties, these pseudopeptidic polycarboxylates are safer and easy-to-synthesize at large scale. The grafted pseudopeptides displayed a pH-responsive coil-to-globule conformational change, which has been shown to trigger membrane destabilization at a value approaching physiological pH.[24-26] They have been successfully employed for intracellular delivery of small molecules, therapeutic protein and siRNA to cells, spheroids and mouse models.[24,27-29] The grafted biopolymers have also been used for intracellular trehalose loading for cell cryopreservation. In particular, PP50 (molar percentage of L-phenylalanine at 50% relative to the pendant carboxylic acid groups on the PLP backbone) was shown to load trehalose into erythrocytes, reaching intracellular trehalose threshold concentrations (100–200 mM) required for bioprotection of mammalian cells in approximately 9 hours.[21,30] However, the long

incubation time required for PP50-mediated trehalose loading is not satisfactory for cell-based therapies which comprise a number of complex processes but usually have a very short time window.[22] On the other hand, the intracellular trehalose delivery efficiency (percentage of intracellular trehalose concentration relative to total trehalose loading concentration) of PP50 was limited to no more than 35%, which resulted in the use of high concentrations of extracellular trehalose for loading.[21,30]

Herein, we report the development of a new approach to achieving very rapid and efficient intracellular delivery of hydrophilic, membrane-impermeable trehalose for enhanced cryopreservation of ovine erythrocytes. Inspired by naturally existing membrane proteins which contain covalently attached long-chain fatty acids acting as membrane anchors, we have recently reported a class of pH-responsive, membrane-anchoring, comb-like pseudopeptides with dramatic endosomolytic activity for efficient cytoplasmic delivery of endocytosed materials through endosomal escape. Through grafting hydrophobic decylamine (NDA) onto carboxylic acid groups pendant to PLP, the comb-like PLP-NDA polymers exhibited the enhanced membrane interaction. In a haemolysis model using erythrocyte membranes as a model for endosomal membranes, the optimal PLP-NDA18 with a degree of NDA substitution at 18 mol% was non membrane-lytic at pH 7.4 but induced nearly complete haemolysis within 20 min upon acidification to late endosomal pH 5.5.[31] However, delivery of membrane-impermeable molecules such as trehalose into erythrocytes (especially ovine erythrocytes whose membranes are more fragile) without causing significant cell damages is notably challenging due to a lack of transduction or endocytosis pathways.[21] In this paper, we investigated the effects of the side chain length, degree of substitution and concentration of the comb-like pseudopeptides with different hydrophobic alkyl side chains, the pH, temperature and time of incubation, as well as the polymer-to-cell ratio and the

concentration of extracellular trehalose in order to achieve very rapid and efficient loading of trehalose into ovine erythrocytes for effective cryopreservation. The haemolytic activity of various delivery formulations was minimized. The mechanism of intracellular delivery mediated by the comb-like pseudopeptides was elucidated, and the enhanced cryopreservation of erythrocytes was demonstrated.

2. Materials and methods

2.1 Materials

Heptylamine (HDA, C7), decylamine (NDA, C10), tetradecylamine (TDA, C14), octadecylamine (ODA, C18), calcein, iso-phthaloyl chloride and anthrone were purchased from Sigma-Aldrich (Dorset, UK). DMSO, *N,N*-dimethylformamide, 4-dimethy-laminopyridine (DMAP) and sodium chloride were obtained from Fisher Scientific (Loughborough, UK). D-(+)-Trehalose dihydrate, L-lysine methyl ester dihydrochloride, ninhydrin, triethylamine and *N,N'*-dicyclohexylcarbodiimide (DCC) were purchased from Alfa Aesar (Heysham, UK). Anhydrous ethanol, acetone, chloroform, hydrochloric acid, sodium hydroxide, methanol, diethyl ether, sodium citrate dehydrate, potassium chloride, potassium dihydrogen orthophosphate and sulfuric acid were obtained from VWR (Lutterworth, UK). Ovine erythrocytes (defibrinated, sterile), which were separated from whole blood by centrifuge and contained no additives, were purchased from TCS Biosciences (Buckingham, UK), stored in a fridge and used within three days of the prescribed four-week shelf life.

2.2 Pseudopeptidic polymer synthesis and characterization

Alkyl chains, such as HDA (C7), NDA (C10), TDA (C14) and ODA (C18), were grafted onto the backbone of the parent pseudopeptidic polymer PLP (M_n = 17.9 kDa, M_w = 35.7 kDa,

polydispersity = 1.99) at various degrees of substitution via DCC/DMAP mediated amide coupling

according to the previously published method.[31] The structures of PLP and the comb-like

pseudopeptides (**Scheme 1**), denoted as PLP-NDA3, PLP-NDA10, PLP-NDA18, PLP-HDA18,

PLP-TDA18 and PLP-ODA18, were confirmed using a Spectrum 100 FT-IR Spectrometer

(PerkinElmer, USA) and a 400 MHz NMR spectrometer (Bruker, Germany). The molecular

weight and polydispersity index (PDI) of PLP (M_w = 35.7 kDa, M_n = 17.9 kDa, PDI = 1.99) were

determined using an aqueous GPC system (Viscotek, UK), which was calibrated with polyethylene

oxide standards according to the previous publication.[23] The actual degrees of substitution of the

comb-like polymers, calculated as the molar percentages of the alkyl side chains relative to the

pendant carboxylic acid groups on the PLP backbone, were determined by the ratio of the integral

0.77-0.91 ppm to the integral 7.45-7.64 ppm in their ^{1}H NMR spectra (**Figure S1**) and used to

calculate their molecular weights. The compositions of these polymers are shown in **Table 1**. The

FT-IR spectra (**Figure S2**) of the pseudopeptidic polymers in their acid forms show characteristic

peaks at 3291 (N–H str and O–H str), 1723 (C=O acid str), 1625 (amide band I), and 1530 cm^{-1}

(amide band II).
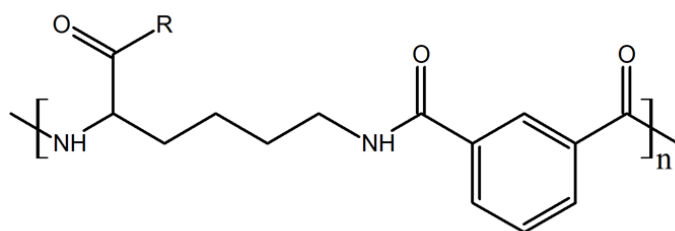
PLP: R = OH
PLP-HDA: R = OH or $NH(CH_2)_6CH_3$
PLP-NDA: R = OH or $NH(CH_2)_9CH_3$
PLP-TDA: R = OH or $NH(CH_2)_{13}CH_3$
PLP-ODA: R = OH or $NH(CH_2)_{17}CH_3$

Scheme 1. Repeat unit structures of PLP, PLP-HDA, PLP-NDA, PLP-TDA and PLP-ODA.

Table 1. Compositions of PLP, PLP-NDA3, PLP-NDA10, PLP-NDA18, PLP-HDA18, PLP-TDA18 and PLP-ODA18.

	PLP	PLP-NDA3	PLP-NDA10	PLP-NDA18	PLP-HDA18	PLP-TDA18	PLP-ODA18
Side chain length (carbon number)	0	10	10	10	7	14	18
Actual degree of substitution (%)	0	3	10	18	18	18	18
M_n (kDa)	17.9	18.2	18.9	19.7	19.1	20.5	21.1

2.3 Trehalose loading

Trehaose solutions were prepared by dissolving trehalose in 306 mOsm phosphate-buffered saline (PBS) at various concentrations and pHs. 0.5 mL of erythrocytes were washed three times with 1 mL of 306 mOsm PBS (pH 7.4), and then resuspended in 1 mL trehalose solution in the presence or absence of the comb-like pseudopeptidic polymers. The resulting erythrocyte samples with a final packed cell volume of 15% were incubated in a shaking water bath (120 rpm) at preset temperature to allow trehalose loading.

2.4 Intracellular trehalose quantification

Anthrone reaction was applied for intracellular trehalose quantitation.[21,30] After trehalose loading, the erythrocyte samples were centrifuged at room temperature and washed twice with 1.5 mL PBS (pH 7.4) iso-osmotic to the incubation mixture to remove extracellular trehalose. The erythrocytes were then mixed with 5 mL 80% (v/v) methanol and incubated in a water bath at 85 °C for 1 h. The samples were centrifuged at 10,500 rpm for 4 min. Their supernatants were collected and then evaporated overnight in an oven at the preset temperature of 100 °C. Each dry residue was dissolved in 2 mL of deionized water. 0.5 mL of the resulting trehalose solution was mixed with 5 mL of 66% (v/v) sulphuric acid containing 0.05% (w/v) anthrone, followed by

incubation at 100 °C for 15 min. The absorbance at 620 nm was measured after sample cooling.

Negative control (erythrocytes incubated in trehalose for less than 1 min to yield negligible trehalose loading) was prepared to determine the anthrone absorbance of residual extracellular trehalose after washing as well as endogenous sugars. Intracellular trehalose concentrations were obtained by comparing to a trehalose concentration versus absorbance standard curve. The trehalose delivery efficiency was then calculated according to the following equation:

$$\text{Delivery efficiency}(\%) = \frac{C_i}{C_t} \times 100$$

where, C_i is the intracellular trehalose concentration after the polymer-mediated delivery and C_t is the total trehalose loading concentration.

2.5 Haemolysis assay

Since haemoglobin oxidation was found to be insignificant during all steps of trehalose loading and erythrocyte cryopreservation[21,30], haemolysis was evaluated by measuring the absorbance of oxyhemoglobin through a simple spectrophotometric method, instead of measuring all forms of haemoglobin.[32] After trehalose loading (or after freezing and thawing), the erythrocyte samples were centrifuged at 3,500 rpm and the absorbance of the supernatant was measured at 541 nm (one of the oxyhemoglobin's absorbance peaks) using a UV-Vis spectrophotometer (GENESYS 10S UV–Vis, Thermo Scientific, USA). Erythrocytes before trehalose loading (or before freezing and thawing) were lysed in deionized water to prepare positive control or resuspended in 306 mOsm PBS buffer alone to prepare negative control. All the measured haemoglobin absorbance was ensured to be in linear relationship with the number of lysed erythrocytes (**Figure S3**). The relative haemolysis was calculated using the following equation:

$$\text{Relative hemolysis (\%)} = \frac{A_s - A_{nc}}{A_{pc}} \times 100$$

where A_s is sample haemoglobin absorbance induced during the experimentation (during trehalose loading or during freezing and thawing), A_{pc} is the positive control haemoglobin absorbance which relates to the initial cell count and A_{nc} is the negative control haemoglobin absorbance which was maintained to be approximately 0.5% relative to positive control.

2.6 Confocal microscopy

Calcein, a membrane impermeable dye, was used as a model payload to investigate the comb-like pseudopeptidic polymer mediated intracellular delivery. Erythrocytes were washed three times with 306 mOsm PBS (pH 7.4) and incubated with 360 mM trehalose, 1 μM calcein, and 0.8 mg mL^{-1} polymer (PP50 or PLP-NDA18) at a specific pH in a shaking water bath (120 rpm, 37°C) for 15 min. Negative control was prepared by incubating erythrocytes with 360 mM trehalose and 1 μM calcein in the absence of polymer at the same specific pH for 15 min. After incubation, the erythrocytes were washed twice with 306 mOsm PBS (pH 7.4) and then imaged using an LSM-510 inverted laser scanning confocal microscope (Zeiss, Germany) at 37°C. Calcein was excited at 488 nm, and the emission at 535 nm was collected.

To assess the erythrocyte membrane integrity after intracellular loading, erythrocytes were incubated with 360 mM trehalose in the presence or absence of pseudopeptidic polymer at pH 6.1 in a shaking water bath (120 rpm, 37°C) for 15 min, followed by washing twice with pH 7.4 PBS. The washed erythrocytes were then resuspended in the pH 7.4 PBS buffer containing 1 μM calcein and imaged using a laser scanning confocal microscope as described above.

2.7 Atomic force microscopy (AFM)

Erythrocytes were washed three times with 306 mOsm PBS (pH 7.4), incubated with 360 mM trehalose solution in the presence or absence of 0.8 mg mL^{-1} pseudopeptidic polymers at pH 6.1 for 15 min, and then immobilized on a polylysine coated microscope slide. The cells were crossed

linked in glutaraldehyde (1%) for 10 min, washed and then air dried.[30] AFM was performed using

an Asylum MFP-3D microscope (Oxford Instruments Asylum Research, US) in tapping mode.

Nanosensors PPP-NCHR tips with resonant frequency around 320 kHz, tip radius 7 nm and spring

constant 42 N m^{-1} were used and tuned to a target tapping amplitude of 1–2 V.

2.8 Cryopreservation

Erythrocytes (15% packed cell volume) were incubated in 360 mM trehalose solution in the

presence or absence of 0.8 mg mL^{-1} PLP-NDA18 at pH 6.1 at 37 °C. After 15 min of incubation,

erythrocytes were washed twice with pH 7.4 PBS buffer iso-osmotic to the incubation solution to

remove PLP-NDA18 and free haemoglobin and reverse membrane permeability. The supernatant

of each erythrocyte sample was then replaced by 360 mM trehalose solution at pH 7.4 yielding a

packed cell volume of approximately 15%. Negative control was prepared by incubating

erythrocytes with PBS (pH 6.1) alone for 15 min, followed by washing and resuspension in PBS

(pH 7.4). 1 mL of the processed erythrocytes were transferred to 2 mL polypropylene cryovials,

directly immersed in liquid nitrogen (cooling rate: 300°C min^{-1}) and then cryopreserved for

specific time periods. Recovery of the cryopreserved erythrocytes was accomplished by thawing

in a water bath at 37°C (thawing rate: 20°C min^{-1}) for 15 min. Immediately after thawing, the

erythrocyte samples were centrifuged at 3,500 rpm for 3 min and the cell pellets were lysed in

deionized water, followed by measurement of haemoglobin absorbance at 541 nm which was

referred to the correlation curve in **Figure S3** to calculate the viable cell number. The cryosurvival

rate was determined by comparing the viable cell number before and after freezing and

thawing.[21,33,34] according to the following equation:

$$\text{Cryosurvival rate (\%)} = \frac{\text{Viable cell number after freezing and thawing}}{\text{Viable cell number before freezing and thawing}} \times 100$$

2.9 Statistical analysis

All data points were repeated in triplicate (n = 3). Results and graphical data are presented as mean values with standard deviation (S.D.) encompassing a 95% confidence interval. Data were analysed for statistical significance by two-tailed Student's t-test.

3. Results and Discussion

3.1. Intracellular trehalose loading by comb-like pseudopeptides

Alkyl side chains have been reported to play an important role as membrane anchors in the enhancement of lipid membrane binding and insertion.[35,36] Four comb-like pseudopeptides, PLP-HDA18, PLP-NDA18, PLP-TDA18 and PLP-ODA18, were synthesized by grafting alkyl side chains of different lengths (C7, C10, C14 and C18, respectively) onto the parent polymer at an actual grafting degree of 18 mol%. The impact of alkyl side chain length on intracellular trehalose delivery and haemolytic activity is shown in **Figure 1**. By slightly increasing the side chain length from 7 to 10 carbons, intracellular trehalose loading was increased by a factor of 2.4. Other researchers have reported that acylation of proteins with longer alkyl side chains can yield stronger membrane association and deeper insertion into the lipid membrane.[37] It has been noted by Mruthy *et al.* that poly(propylacrylic acid) with one additional methylene unit in the pendant alkyl group showed stronger membrane disruption than poly(α-ethylacrylic acid).[38] **Figure 1** shows that with increasing alkyl side chain length over 10 carbons, intracellular trehalose loading was reduced significantly. This is because an increase in alkyl chain length can remarkably enhance polymer hydrophobicity, which if too high could cause polymer aggregation and consequently reduce polymer-membrane interaction.[37,39] PLP-NDA18 containing 10-carbon alkyl side chains was found to be superior, resulting in an intracellular trehalose concentration of 177.9 ± 8.6 mM after only

15 min of incubation. Intracellular trehalose concentrations between 100 and 200 mM have been found to achieve favorable cryoprotection of mammalian cells including murine fibroblasts and human oocytes and keratinocytes.[15,40] In contrast, Holovati *et al*. have reported that the intracellular trehalose concentration (below 15 mM) loaded by liposomes was too low to achieve improved cryoprotection of erythrocytes.[20]
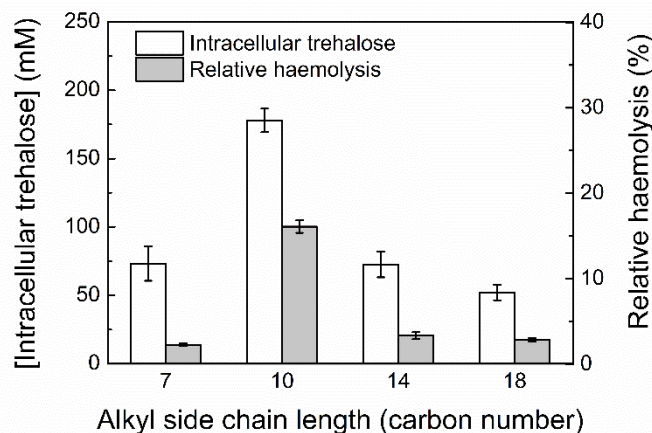
Figure 1. Impact of alkyl side chain length at a fix degree of substitution of 18 mol% on intracellular trehalose concentration and relative haemolysis. Erythrocytes were incubated with the PBS buffer solution containing 360 mM trehalose and 0.8 mg mL^{-1} pseudopeptide for 15 min. Temperature = 37°C; pH = 6.1. Mean ± S.D. (n = 3).

Three membrane-anchoring, comb-like pseudopeptides containing hydrophobic relatively long NDA side chains, PLP-NDA3, PLP-NDA10 and PLP-NDA18 (actual degree of grafting at 3, 10 and 18 mol% respectively), were employed to facilitate intracellular delivery of membrane-impermeable trehalose. The intracellular trehalose concentration and haemolytic activity were shown to increase with increasing the degree of grafting with NDA side chains (**Figure 2**). The intracellular trehalose concentration of 177.9 ± 8.6 mM induced by PLP-NDA18 was 3.9 times

more efficient than PLP-NDA3 after 15 min of incubation. This is attributed to our previous finding that increasing the degree of grafting with NDA side chains can significantly enhance polymer hydrophobicity, leading to considerably enhanced polymer-membrane interaction and intracellular delivery.[31] PLP-NDA18 was the most favourable for intracellular trehalose delivery, with high delivery efficiency but only marginally increased haemolysis.
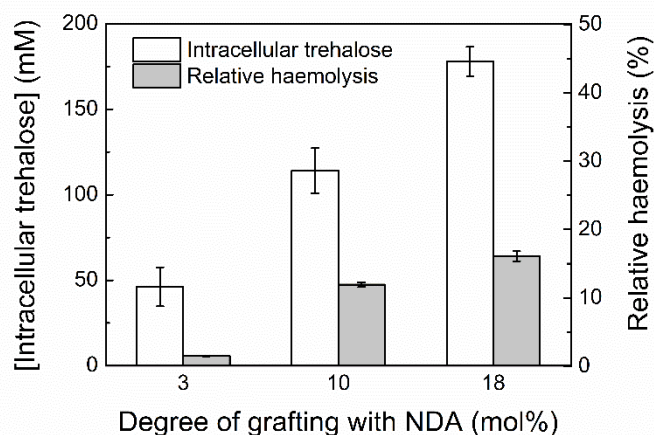
Figure 2. Impact of degree of grafting with NDA on trehalose loading and relative haemolysis. Erythrocytes were incubated with the PBS buffer solution containing 360 mM trehalose and 0.8 mg mL^{-1} pseudopeptide for 15 min. Temperature = 37°C; pH = 6.1. Mean ± S.D. (n = 3).

3.2. Characterisation of PLP-NDA18 mediated trehalose loading

The amount of membrane-impermeable trehalose delivered intracellularly by the comb-like pseudopeptides is a function of parameters such as polymer concentration, extracellular pH, incubation temperature, and extracellular trehalose concentration. These were investigated to optimise intracellular trehalose loading.

3.2.1. Impact of polymer concentration

The intracellular trehalose concentration and relative haemolysis increased with increasing the concentration of PLP-NDA18 within the range of 0.3–0.8 mg mL^{-1} at pH 7.05 (**Figure 3A**). The intracellular trehalose concentration (129.5 ± 15.6 mM) achieved after 15 min of incubation with 0.8 mg mL^{-1} PLP-NDA18 at pH 7.05 was 1.4 times lower compared to the treatment at pH 6.1. **Figures S4** and **S5** show that intracellular trehalose loading was enhanced with extending the incubation time to 30 and 60 min respectively, but with concomitant increase in haemolysis. No significant enhancement of intracellular trehalose concentration ($P > 0.5$) was observed with further increasing the polymer concentration from 0.8 to 1.2 mg mL^{-1} (**Figure 3A**), indicating that maximum permeability to trehalose was induced by PLP-NDA18. The concentration-dependent trehalose loading profile is in good agreement with the reports that increasing polymer concentration can enhance the driving force for membrane binding, leading to enhanced membrane permeability.[24,25,41]

3.2.2. Impact of extracellular pH

As shown in **Figure 3B**, significant intracellular trehalose loading was observed at pH 7.05 and further enhanced with decreasing pH to 5.6 for the incubation of erythrocytes with all the three concentrations (0.6, 0.8 and 1.2 mg mL^{-1}) of PLP-NDA18 for 15 min. The most significant enhancement in intracellular trehalose loading was observed upon reduction of pH from 6.5 to 6.1 where maximum intracellular treahlose concertation was reached. This finding is attributed to enhanced polymer hydrophobicity resulting from side-chain modification with hydrophobic relatively long NDA. With decreasing pH, carboxyl groups pendant to the pseudopeptides were protonated and the hydrophobic interaction became predominant, resulting in a transition of polymer conformation from expanded coils to collapsed globular structures with considerably enhanced membrane interaction.[24,25,31]

It is worth pointing out that relative haemolysis of the ovine erythrocytes treated with trehalose in the presence of 0.6, 0.8 and 1.2 mg mL^{-1} PLP-NDA18 within the pH range 5.6–7.05 for 15 min were all below 20%, with negligible changes in response to pH (**Figure S6**). In contrast, in our previous haemolysis model using erythrocyte membranes as a model for endosomal membranes, ovine erythrocytes treated with 0.5 mg mL^{-1} PLP-NDA18 at pH 5.5 displayed a considerably higher level of haemolysis at 72.8 ± 1.8% after 10 min and reached nearly complete haemolysis after 20 min through pore formation.[31] This huge difference in haemolytic activity was attributed to different polymer-to-cell ratios. The polymer-to-cell ratio in this trehalose-loading study was carefully optimized to be over 40 times lower than the one used in our previous haemolysis model for the study of endosomolytic activity. Use of the tremendously lower polymer-to-cell ratio (readily achievable by increasing the cell density at a fixed polymer concentration) ensured marginal haemolysis but still yielded favorable membrane permeabilization to allow very rapid and efficient trehalose loading into ovine erythrocytes. This successfully addressed the major challenge on delivery of membrane-impermeable molecules into erythrocytes lacking transduction or endocytosis pathways without causing significant cell death.[21] Other researchers have reported a similar observation that the content leakage from liposomes caused by melittin was reduced with decreasing peptide-to-lipid ratio.[42,43]
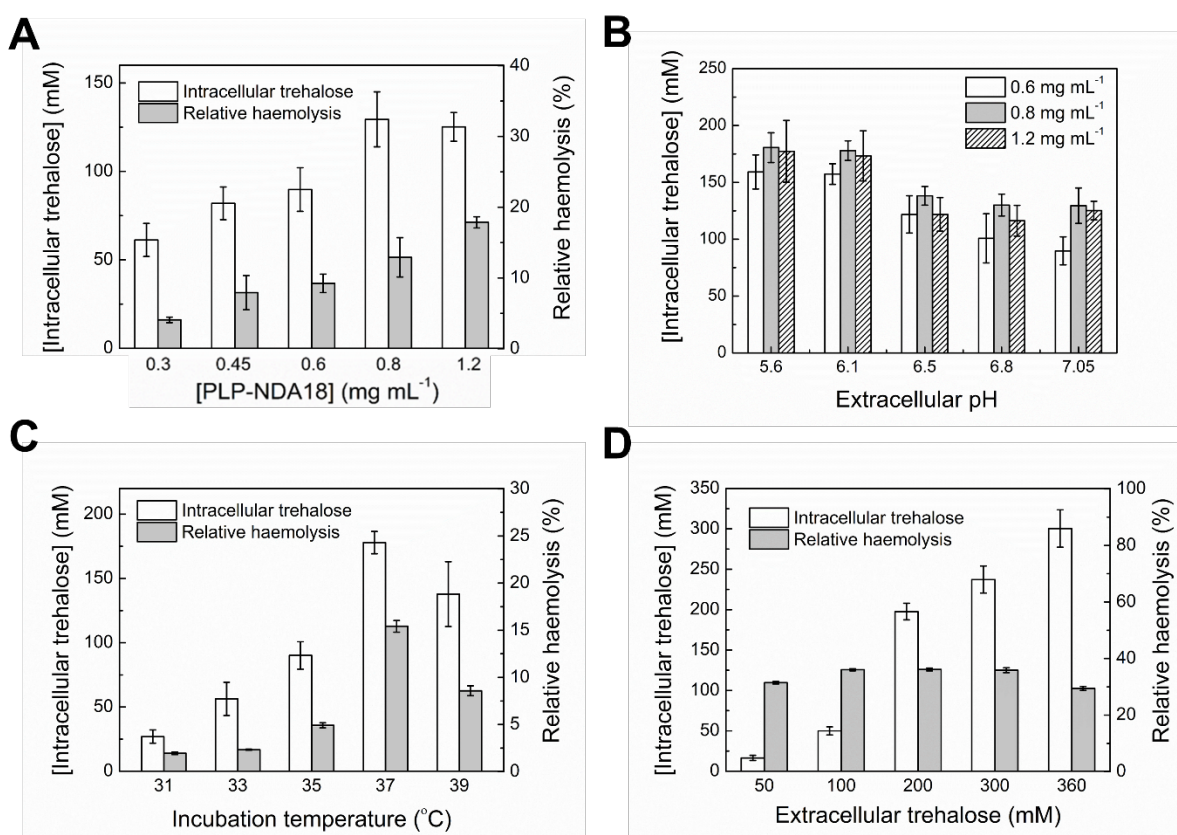
3.2.3. Impact of incubation temperature

Figure 3C shows that intracellular trehalose loading and relative haemolysis were dependent on incubation temperature. After 15 min of incubation in a water bath at 31°C, a low intracellular trehalose concentration of 27.0 ± 5.2 mM was detected. Once increasing incubation temperature to 37°C, the intracellular trehalose concentration increased by a factor of 6.5. This is likely due to the fact that the phase behaviour and physical properties of erythrocyte membrane lipids are

extremely sensitive to temperature changes.[44] At physiological temperature (37°C), the cell membrane is more fluid, which may contribute to the enhanced polymer-lipid interaction and the consequent increased intracellular delivery.[21,45] In addition, intracellular loading could be further improved by the higher diffusion rate of molecules at higher temperature.[21] However, increasing incubation temperature from 37°C to 39°C reduced trehalose loading, which might be due to the reduced polymer-membrane interaction caused by the formation of lipid devoid domains on the cell membrane surface once exceeding the physiological temperature.[46]

3.2.4. Impact of extracellular trehalose concentration

A higher extracellular trehalose concentration has been reported to cause a higher osmotic imbalance across the cell membrane, which as a result can create a higher driving force to achieve improved intracellular delivery.[45] **Figure 3D** depicts the impact of extracellular trehalose concentration on intracellular trehalose loading. In the presence of 0.8 mg mL^{-1} PLP-NDA18 at pH 6.1 for 60 min, intracellular trehalose loading was enhanced dramatically by a factor of 18.3 from 16.4 ± 3.2 to 300.3 ± 23.2 mM with increasing the external trehalose concentration from 50 to 360 mM, respectively. In contrast, Lynch *et al*. has reported a 2.4 times lower intracellular trehalose concentration after 9 times longer incubation of ovine erythrocytes with PP50 pendanted with L-phenylalanine and 360 mM extracellular trehalose.[21] It is also interesting to note that the relative haemolysis after 60 min of co-incubation of erythrocytes with PLP-NDA18 and trehalose within the concentration range tested was kept below approximately 30% with limited variations. As comparison, relative haemolysis in the presence of PP50 was decreased with increasing extracellular trehalose concentration.[21] It has been reported that PP50 and hydrophilic dextran (polysaccharide of glucose) were present in a mixture with no obvious formation of complexes, suggesting limited interaction between the two components.[47] Similarly, PP50 would have limited

interaction with hydrophilic trehalose (disaccharide of glucose), but it was argued that surrounding

of PP50 by high concentrations of trehalose could inhibit its conformational change to hydrophobic

compact polymer structures at mildly acidic pH, leading to inhibition of its membrane interaction

and consequent reduction of trehalose loading and haemolysis.[21] Other researchers have reported

similar observations on inhibition of peptide folding by high concentrations of trehalose, which

can thickly cluster around constituent amino acids and shield them from each other.[48] As

comparison, such shielding effect of hydrophilic trehalose on the comb-like pseudopeptide, PLP-

NDA18, was diminished likely due to enhanced polymer hydrophobicity and its comb-like

structure containing hydrophobic relatively long NDA side chains. Therefore, PLP-NDA18 well

retained its membrane-permeabilizing activity in the presence of high concentrations of trehalose,

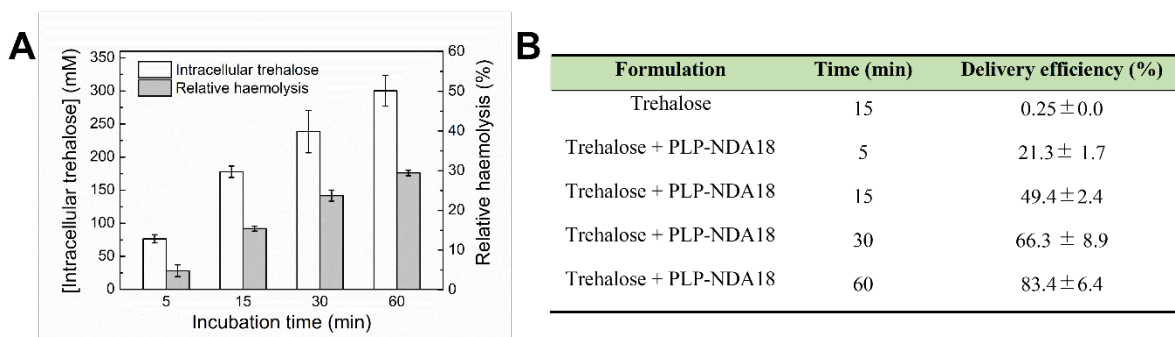maintaining very rapid and efficient intracellular trehalose loading.

Figure 3. Optimization of PLP-NDA18 mediated intracellular trehalose loading. (A) Impact of PLP-NDA18 concentration on intracellular trehalose concentration and relative haemolysis. Erythrocytes were incubated with the PBS buffer containing 360 mM trehalose and different concentrations of PLP-NDA18 for 15 min. Temperature = 37°C, pH = 7.05. (B) Impact of extracellular pH on trehalose loading. Erythrocytes were incubated with the PBS buffer containing 360 mM trehalose and 0.6, 0.8 and 1.2 mg mL^{-1} PLP-NDA18 at various pHs at 37°C for 15 min. (C) Impact of incubation temperature on trehalose loading and relative haemolysis. Immediately after erythrocytes were suspended in the PBS buffer (pH 6.1) containing 360 mM trehalose and 0.8 mg mL^{-1} PLP-NDA18, the sample was quickly immersed in a temperature-controlled water bath for 15 min at different incubation temperatures. (D) Impact of extracellular trehalose concentration on intracellular trehalose delivery and relative haemolysis. Erythrocytes were incubated with the PBS buffer containing different concentrations of trehalose and 0.8 mg mL^{-1} PLP-NDA18 for 60 min. Temperature = 37°C, pH = 6.1. Mean ± S.D. (n = 3).

3.3. Intracellular trehalose delivery efficiency and kinetics

Figure 4 shows very rapid and efficient intracellular trehalose loading facilitated by 0.8 mg mL^{-1} PLP-NDA18 at pH 6.1 and 37°C. Upon incubation of erythrocytes with 360 mM trehalose alone for 15 min, the intracellular concertation (0.9 ± 0.1 mM) of the membrane-impermeable, hydrophilic compound was extremely low and the calculated delivery efficiency was only 0.25 ± 0.0%. As comparison, 76.5 ± 6.2 mM trehalose (delivery efficiency 21.3 ± 1.7%) was very rapidly loaded into erythrocytes by PLP-NDA18 after incubation for only 5 min. Intracellular trehalose loading and relative haemolysis increased with increasing incubation time. When the incubation time was extended from 15 to 60 min, the intracellular trehalose concentration achieved by PLP-

NDA18 increased from 177.9 ± 8.6 mM (delivery efficiency 49.4 ± 2.4%) to 300.3 ± 23.2 mM (delivery efficiency 83.4 ± 6.4%), with the latter 334 times higher than that in the absence of PLP-NDA18.

PP50 pendanted with L-phenylalanine was previously reported to enable enhanced intracellular trehalose loading for effective cell cryopreservation.[21,30,33] However, it is a considerably less efficient trehalose loading process with a considerably lower loading rate compared to the PLP-NDA18 mediated trehalose loading. It has been previously reported that only approximately 10 mM trehalose (delivery efficiency around 2.8%) was loaded into erythrocytes after 1.5 h of co-incubation with PP50[21], which was 30-fold less efficient than trehalose loading by the comb-like PLP-NDA18 pendanted with hydrophobic relatively long alkyl chains after 1 h of treatment. In order to increase the intracellular trehalose concentration to thresholds (100-200 mM) required for cellular bioprotection during preservation[15,36], 9 h of treatment was usually required for PP50 to result in an intracellular trehalose concentration at 123 ± 16 mM (delivery efficiency 34.2%).[21] As comparison, 177.9 ± 8.6 mM trehalose (delivery efficiency 49.4 ± 2.4%) was loaded into erythrocytes by PLP-NDA18 after only 15 min of treatment (**Figure 4**), suggesting that its intracellular delivery rate was approximately 36 times higher than PP50. Therefore, for effective cryopreservation in this work, a short co-incubation of ovine erythrocytes with PLP-NDA18 and trehalose for no more than 15 min was chosen and haemolysis was below 16.1 ± 0.7%.

| Formulation	Time (min)	Delivery efficiency (%)
Trehalose	15	0.25±0.0
Trehalose + PLP-NDA18	5	21.3± 1.7
Trehalose + PLP-NDA18	15	49.4±2.4
Trehalose + PLP-NDA18	30	66.3 ± 8.9
Trehalose + PLP-NDA18	60	83.4±6.4

Figure 4. (A) Time-dependent intracellular trehalose loading and relative haemolysis mediated by PLP-NDA18. (B) Comparison of delivery efficiency. Erythrocytes were treated with the PBS containing 360 mM trehalose in the absence or presence of 0.8 mg mL^{-1} PLP-NDA18 for specific time periods. Temperature = 37°C; pH = 6.1. Mean ± S.D. (n = 3).

3.4. Reversibility and mechanism of membrane permeabilization

The binary mixture of trehalose and calcein, which are both membrane-impermeable, was used to compare the intracellular delivery by the comb-like PLP-NDA18 polymer pendanted with 10-carbon NDA chains and the grafted PP50 polymer pendanted with L-phenylalanine. As shown in **Figure 5A**, after incubation at pH 7.4 for 15 min, no green calcein fluorescence was observed in erythrocytes with or without polymer treatment, indicating that at physiological pH neither PLP-NDA18 nor PP50 was membrane permeabilizing. After incubation at pH 6.1 for 15 min, strong homogenous green fluorescence was only observed in the erythrocytes treated with PLP-NDA18, whilst there was no detectable intracellular green fluorescence for the PP50-treated erythrocyte sample. This consolidates our finding that PLP-NDA18 can mediate considerably more rapid and more efficient intracellular delivery than PP50.

However, after erythrocytes were pre-treated with trehalose and PLP-NDA18 at pH 6.1 for 15 min and then washed with pH 7.4 PBS, the subsequent incubation of erythrocytes with calcein alone did not result in detectable intracellular green fluorescence, which was indistinguishable from the erythrocyte sample with pre-treatment in the absence of PLP-ND18 (**Figure 5B**). This indicates that washing with pH 7.4 PBS as a quenching buffer quickly reversed the cell membrane permeability and PLP-NDA18 did not cause permanent alteration of the membrane integrity. Accordingly, the loaded trehalose became locked inside erythrocytes after the immediate post-

loading washing step (**Figure 5A**). This is because washing in the PBS buffer at physiological pH can not only act to physically remove PLP-NDA18 from erythrocytes but also switch off its membrane permeabilizing activity. Similar observations have been reported on the reversible membrane permeability achieved by amphiphilic peptides[43] and the PP50 polymer[21].
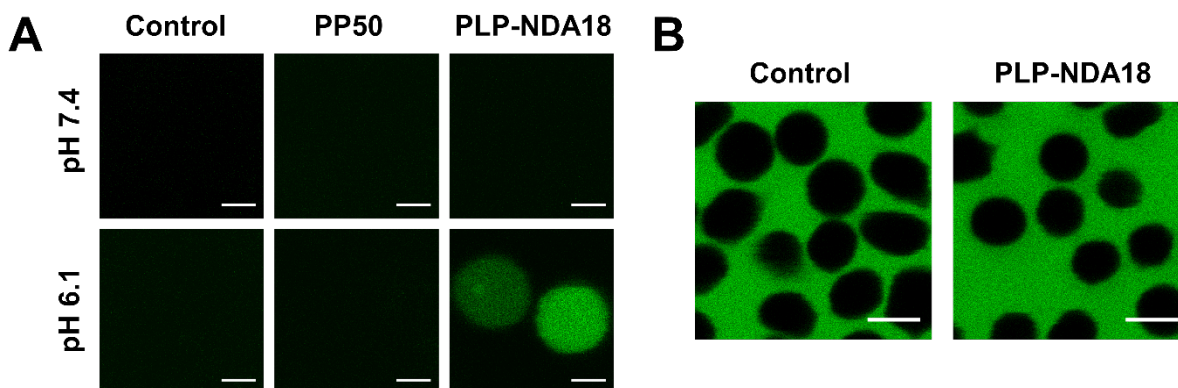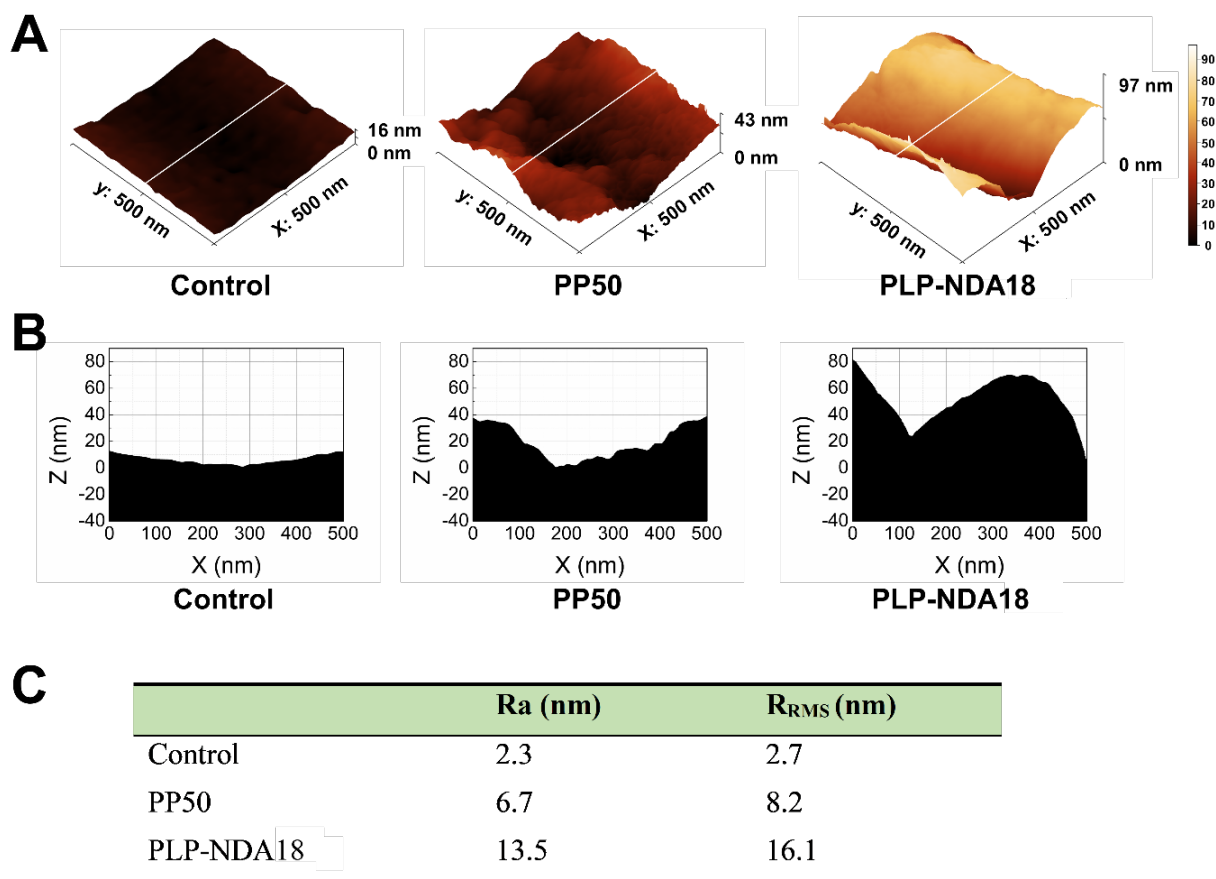

Figure 5. (A) Confocal microscopy images of polymer-mediated delivery into erythrocytes. Erythrocytes were co-incubated with 360 mM trehalose and 1 μM calcein in the absence (control) or presence of 0.8 mg mL^{-1} polymer (PP50 or PLP-NDA18) for 15 min; pH = 7.4 or 6.1; temperature = 37°C. Erythrocytes were washed with pH 7.4 PBS before imaging. Scale bar: 2 μm. (B) Investigation of reversibility of membrane permeability. Erythrocytes were incubated with 360 mM trehalose in the absence (control) or presence of 0.8 mg mL^{-1} PLP-NDA18 at pH 6.1 for 15 min, followed by washing with pH 7.4 PBS buffer and then treatment with pH 7.4 PBS containing 1 μM calcein before imaging. Scale bar: 4 μm.

AFM was applied to visualize the polymer-membrane interaction at mildly acidic pH. **Figures 6A** and **S7** show surface morphologies of the erythrocyte membrane treated with PBS alone, PP50 and PLP-NDA18 at pH 6.1, respectively. Obvious membrane deformation was observed in the erythrocytes treated with PP50 or PLP-NDA18 compared to the control. The line profiles (**Figure**

6B) suggest that both PP50 and PLP-NDA18 created depressions on the erythrocyte surface. Instead of gradually and uniformly thinning the lipid membrane, distinct domains with significantly increased curvatures were formed by both amphiphilic pseudopeptides. It has been reported that some proteins, such as epsin, endophilin and amphiphysin, can also induce a similar membrane curvature change through the insertion of their amphiphilic domains into the membrane bilayer and the reduced hydrophobicity of amino acids in such domains may impair their ability to produce membrane curvature.[49] The inserted hydrophobic protein motifs in the outer part of the lipid membrane can serve as a "wedge", perturbing the lipid packing and thus causing membrane bending.[50] In this paper, PLP-NDA18 containing relatively long alkyl side chains caused the deeper and sharper erythrocyte surface depression (**Figure 6B**) and a consequent 2-fold increase in the surface roughness as compared to PP50 with phenylalanine side chains (**Figure 6C**). It is consistent with a report that alkyl chains play a more important role in binding of peptides with the lipid membrane than phenylalanine.[51] The stronger membrane binding and insertion of PLP-NDA18 produced the more pronounced membrane curvature. This is in good agreement with the observations reported by other researchers that several insertions into the lipid membrane held in close proximity may result in high membrane curvatures.[50,52] As a consequence, stronger membrane stresses can be generated by higher curvatures, leading to more significant cell deformation[50,53] and the subsequently higher membrane permeability for improved intracellular delivery[54,55]. In addition, compared to PP50, the more pronounced membrane curvature induced by PLP-NDA18 might also result in a higher number of membrane-thinning domains, which was demonstrated to play a key role in PP50 mediated intracellular delivery.[30] Therefore, all these could contribute to the tremendously more rapid and efficient intracellular trehalose delivery of PLP-NDA18 than PP50. Compared with other membrane stress based intracellular delivery

technologies which rely on mechanical perturbations or shear forces provided by specifically designed equipment[6], the comb-like pseudopeptides can enable efficient, controllable, cost-effective and readily scalable intracellular delivery. Also importantly, the PLP-NDA18 induced membrane bending and destabilization is transient and reversible (**Figure 5**), thus eliminating safety concerns.

A

Control — PP50 — PLP-NDA18

B

Control — PP50 — PLP-NDA18

C

	Ra (nm)	R_{RMS} (nm)
Control	2.3	2.7
PP50	6.7	8.2
PLP-NDA18	13.5	16.1

Figure 6. (A) Topographic AFM micrographs and (B) line profiles of the erythrocyte membrane surface treated with PBS alone (control), 0.8 mg mL^{-1} pseudopeptide pendanted with L-phenylalanine (PP50), or 0.8 mg mL^{-1} pseudopeptide pendanted with NDA alkyl chains (PLP-NDA18) at pH 6.1 for 15 min, temperature = 37°C. (C) Average roughness (R_a) and root mean

squared roughness (R_{RMS}) of the erythrocyte membrane surface treated with the same conditions, as determined by AFM.

3.5. Cryopreservation of erythrocytes

A short co-incubation of ovine erythrocytes with 0.8 mg mL^{-1} PLP-NDA18 and 360 mM trehalose at pH 6.1 and 37°C for only 15 min efficiently resulted in the intracellular trehalose at 177.9 ± 8.6 mM, reaching thresholds (100-200 mM) required for cellular bioprotection during preservation[15,36], but yielded the low haemolysis of 16.1 ± 0.7%. This has prompted an evaluation of the trehalose method for cryopreservation of ovine erythrocytes.

In order to examine the effect of trehalose present both inside and outside erythrocytes on cryoprotection, the post freeze-thaw survival rate of erythrocytes co-incubated with trehalose and PLP-NDA18 was compared to the cryosurvival rate of erythrocytes incubated with trehalose alone. Fast freezing and thawing rates have been found to be favourable for cryoprotection of erythrocytes employing trehalose and other carbohydrates.[21,56] Herein, freezing through direct immersion in liquid nitrogen (cooling rate: 300°C min^{-1}) followed by thawing in a water bath at 37°C (thawing rate: 20°C min^{-1}) was chosen as the cryopreservation protocol.

Figure S8 shows that cryosurvival of erythrocytes suspended in PBS alone was negligible. As seen in **Figure 7**, in the presence of extracellular trehalose alone, 69.4 ± 0.4% erythrocytes survived freeze-thaw after 1 h of cryostorage in liquid nitrogen. This is consistent with a previous report that trehalose not only inhibited the formation of extracellular ice crystals through vitrification but also inhibited the formation of intracellular ice crystals via partial dehydration of cells before freezing.[57] As comparison, the cryosurvival rate of erythrocytes with both extracellular and intracellular trehalose increased significantly (P < 0.001) to 90.3 ± 0.7% after cryostorage for

1 h. Almost no variation was observed in the cryosurvival rate of erythrocytes after extended

cryostorage in liquid nitrogen to 7 days.
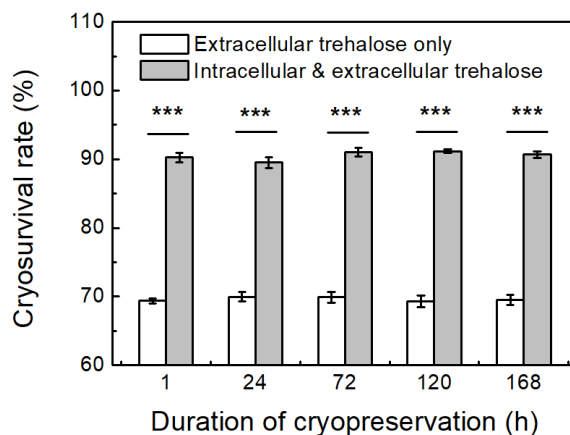
Figure 7. Time-dependent cryosurvival rates of erythrocytes suspended in only 360 mM

extracellular trehalose solution yielding no significant intracellular trehalose loading, and

erythrocytes loaded with 177.9 ± 8.6 mM intracellular trehalose and suspended in 360 mM

extracellular trehalose. Trehalose loading was achieved by incubation of erythrocytes with 360

mM trehalose in the absence or presence of 0.8 mg mL^{-1} PLP-NDA18 at pH 6.1 and 37°C for 15

min. Mean ± S.D. (n = 3), ***P < 0.001.

Non-toxic trehalose is a more attractive bioprotectant for cryopreservation of erythrocytes

compared to the widely used glycerol method which requires deglycerolization after thawing to

avoid post-transfusion osmotic haemolysis.[10-12,58] However, it is notably challenging to deliver

membrane-impermeable hydrophilic trehalose into mammalian cells, especially erythrocytes

lacking transduction or endocytosis pathways,[21] in an efficient and non-invasive way. This remains

a major hurdle to utilizing trehalose as an alternative cryoprotective agent. This paper reports the

first-known cryopreservation of erythrocytes based on very rapid and efficient trehalose loading

by pH-responsive, comb-like pseudopeptides. Intracellular trehalose threshold concentrations (100–200 mM) can be achieved within no more than 15 min through reversible membrane permeability to enable the enhanced erythrocyte cryopreservation. Further investigation into post-thawing cell recovery, including cell morphology, deformability, osmotic fragility, protein and lipid oxidation, enzymatic activities and shelf-life, remains to be carried out. This trehalose method also has potential for preservation of nucleated cells, which currently relies on the use of toxic dimethyl sulfoxide (DMSO) at high concentrations. Furthermore, the comb-like pseudopeptides also have potential for intracellular delivery of other membrane-impermeable, hydrophilic molecules.

4. Conclusion

A very rapid and efficient intracellular delivery method was developed based on reversible cell membrane permeabilization via utilization of the pH-responsive, comb-like pseudopeptides pendanted with relatively long alkyl chains acting as membrane anchors. The intracellular delivery of membrane-impermeable trehalose was dependent on the side chain length, degree of substitution and concentration of the polymers, the pH, temperature and time of incubation, as well as the polymer-to-cell ratio and the concentration of extracellular trehalose. Under optimized conditions, PLP-NDA18 loaded 177.9 ± 8.6 mM trehalose into erythrocytes, which resulted in 90.3 ± 0.7% erythrocyte survival after freeze-thaw, with an improvement of 20.9% in cryosurvival over the erythrocytes suspended in only extracellular trehalose. Compare to the previously reported PP50 pendanted with L-phenylalanine, the comb-like PLP-NDA18 tremendously shortened the loading time from 9 h to 15 min, whilst achieved the higher intracellular trehalose concentration and better erythrocyte cryosurvival. The more rapid and efficient intracellular delivery of PLP-

NDA18 was attributed to the more pronounced membrane curvature generated by the stronger membrane insertion of the comb-like polymer with relatively long alkyl side chains. This new method not only opens an avenue for effective cryopreservation of erythrocytes and potentially other mammalian cells, but also provide a foundation for efficient intracellular delivery of other membrane-impermeable molecules.

ASSOCIATED CONTENT

Supporting Information

^{1}H-NMR and FT-IR spectra of PLP, PLP-HDA18, PLP-NDA18, PLP-TDA18 and PLP-ODA18, linear correlation curve between the erythrocyte concentration and haemoglobin absorbance at 541 nm, impact of PLP-NDA18 concentrations on trehalose loading and relative haemolysis after treatment of erythrocytes for 30 and 60 min, pH-dependent relative haemolysis of erythrocytes treated with trehalose and PLP-NDA18, topography, tapping amplitude and tapping phase images of the erythrocyte membrane surface treated with PBS, PP50 or PLP-NDA18 at pH 6.1 for 15 min, as well as time-dependent cryosurvival rates of erythrocytes suspended in PBS.

AUTHOR INFORMATION

Corresponding Author

* Tel: +44 (0)20 75942070. Fax: +44 (0)20 75945638. Email: rongjun.chen@imperial.ac.uk (R.C.)

Author Contributions

‡S.C. and L. W. contributed equally.

All authors have read, commented on, and approved the final version of the paper.

Notes

A UK patent application (No. 1612150.1) related to poly (L-lysine isophthalamide) (PLP) polymers

with hydrophobic pendant chains has been filed and led to a PCT application (No. WO 2018/011580). R.C., S.C. and L.W. are listed as inventors and declare financial interest with AlphaCells Biotechnologies Limited, a company that may be affected by the research reported in the enclosed paper. All other authors declare no competing interests.

ACKNOWLEDGMENTS

REFERENCES

(1)   Yoo, J. W.; Irvine, D. J.; Discher, D. E.; Mitragotri, S. Bio-Inspired, Bioengineered and Biomimetic Drug Delivery Carriers. *Nat. Rev. Drug Discov.* **2011**, *10* (7), 521–535.

(2)   Mitragotri, S.; Burke, P. A.; Langer, R. Overcoming the Challenges in Administering Biopharmaceuticals: Formulation and Delivery Strategies. *Nat. Rev. Drug Discov.* **2014**, *13* (9), 655–672.

(3)   Yin, H.; Kanasty, R. L.; Eltoukhy, A. A.; Vegas, A. J.; Dorkin, J. R.; Anderson, D. G. Non-Viral Vectors for Gene-Based Therapy. *Nat. Rev. Genet.* **2014**, *15* (8), 541–555.

(4)   Lu, Y.; Sun, W.; Gu, Z. Stimuli-Responsive Nanomaterials for Therapeutic Protein Delivery. *J. Control. Release* **2014**, *194*, 1–19.

(5)   Kanias, T.; Acker, J. P. Mammalian Cell Desiccation: Facing The Challenges. *Cell Preserv.*
        Technol. **2006**, *4* (4), 253–277.

(6)   Stewart, M. P.; Sharei, A.; Ding, X.; Sahay, G.; Langer, R.; Jensen, K. F. In Vitro and Ex
        Vivo Strategies for Intracellular Delivery. *Nature* **2016**, *538* (7624), 183–192.

(7)   Scott, K. L.; Lecak, J.; Acker, J. P. Biopreservation of Red Blood Cells: Past, Present, and
        Future. *Transfus. Med. Rev.* **2005**, *19* (2), 127–142.

(8)   Hod, E. A. Macrophage Recycling of Red Blood Cells and Iron Following Transfusion.
        Blood **2018**, *132* (Suppl 1), SCI-3.

(9)   Flegel, W. A.; Natanson, C.; Klein, H. G. Does Prolonged Storage of Red Blood Cells Cause
        Harm? *Br. J. Haematol.* **2014**, *165* (1), 3–16.

(10)   Klein, H. G.; Spahn, D. R.; Carson, J. L. Red Blood Cell Transfusion in Clinical Practice.
        Lancet **2007**, *370* (9585), 415–426.

(11)   Mitchell, D. E.; Lovett, J. R.; Armes, S. P.; Gibson, M. I. Combining Biomimetic Block
        Copolymer Worms with an Ice-Inhibiting Polymer for the Solvent-Free Cryopreservation
        of Red Blood Cells. *Angew. Chemie* **2016**, *128* (8), 2851–2854.

(12)   Crowe, J. H.; Crowe, L. M. Preservation of Mammalian Cells—Learning Nature's Tricks.
        Nat. Biotechnol. **2000**, *18* (2), 145–146.

(13)   Notman, R.; Noro, M.; O'Malley, B.; Anwar, J. Molecular Basis for Dimethylsulfoxide
        (DMSO) Action on Lipid Membranes. *J. Am. Chem. Soc* **2006**, *128* (43), 13982–13983.

(14)   Rao, W.; Huang, H.; Wang, H.; Zhao, S.; Dumbleton, J.; Zhao, G.; He, X. Nanoparticle-Mediated Intracellular Delivery Enables Cryopreservation of Human Adipose-Derived Stem Cells Using Trehalose as the Sole Cryoprotectant. *ACS Appl. Mater. Interfaces* **2015**, *7* (8), 5017–5028.

(15)   Eroglu, A.; Russo, M. J.; Bieganski, R.; Fowler, A.; Cheley, S.; Bayley, H.; Toner, M. Intracellular Trehalose Improves the Survival of Cryopreserved Mammalian Cells. *Nat. Biotechnol.* **2000**, *18* (2), 163–167.

(16)   Ali Eroglu; Lawitts, J. A.; Toner, M.; Toth, T. L. Quantitative Microinjection of Trehalose into Mouse Oocytes and Zygotes, and Its Effect on Development. *Cryobiology* **2003**, *46* (2), 121–134.

(17)   Shirakashi, R.; Köstner, C. M.; Müller, K. J.; Kürschner, M.; Zimmermann, U.; Sukhorukov, V. L. Intracellular Delivery of Trehalose into Mammalian Cells by Electropermeabilization. *J. Membr. Biol.* **2002**, *189* (1), 45–54.

(18)   Chen, T.; Acker, J. P.; Bayley, A. E. S. C. H.; Fowler, A.; Toner, M. Beneficial Effect of Intracellular Trehalose on the Membrane Integrity of Dried Mammalian Cells. *Cryobiology* **2001**, *43* (2), 168–181.

(19)   Guo, N.; Puhlev, I.; Brown, D. R.; Mansbridge, J.; Levine, F. Trehalose Expression Confers Desiccation Tolerance on Human Cells. *Nat. Biotechnol.* **2000**, *18* (2), 168–171.

(20)   Holovati, J. L.; Gyongyossy-Issa, M. I. C.; Acker, J. P. Effects of Trehalose-Loaded Liposomes on Red Blood Cell Response to Freezing and Post-Thaw Membrane Quality. *Cryobiology* **2009**, *58* (1), 75–83.

(21)   Lynch, A. L.; Chen, R.; Dominowski, P. J.; Shalaev, E. Y.; Yancey, R. J.; Slater, N. K. H.; Yancey Jr, R. J.; Slater, N. K. H. Biopolymer Mediated Trehalose Uptake for Enhanced Erythrocyte Cryosurvival. *Biomaterials* **2010**, *31* (23), 6096–6103.

(22)   Chen, S.; Ren, J.; Chen, R. Cryopreservation and Desiccation Preservation of Cells. In *Comprehensive Biotechnology 3rd edition*; Moo-Young, M., Ed.; Elsevier: Amsterdam, 2019, 5, 157–166.

(23)   Chen, R.; Eccleston, M. E.; Yue, Z.; Slater, N. K. H. Synthesis and pH-Responsive Properties of Pseudo-Peptides Containing Hydrophobic Amino Acid Grafts. *J. Mater. Chem.* **2009**, *19* (24), 4217–4224.

(24)   Chen, R.; Khormaee, S.; Eccleston, M. E.; Slater, N. K. H. The Role of Hydrophobic Amino Acid Grafts in the Enhancement of Membrane Disruptive Activity of pH-Responsive Pseudo-Peptides. *Biomaterials* **2009**, *30* (10), 1954–1961.

(25)   Chen, R.; Khormaee, S.; Eccleston, M. E.; Slater, N. K. H. Effect of L-Leucine Graft Content on Aqueous Solution Behavior and Membrane-Lytic Activity of a PH-Responsive Pseudopeptide. *Biomacromolecules* **2009**, *10* (9), 2601–2608.

(26)   Zhang, S.; Nelson, A.; Coldrick, Z.; Chen, R. The Effects of Substituent Grafting on the Interaction of pH-Responsive Polymers with Phospholipid Monolayers. *Langmuir* **2011**, *27* (13), 8530–8539.

(27)   Ho, V. H. B.; Slater, N. K. H.; Chen, R. pH-Responsive Endosomolytic Pseudo-Peptides for Drug Delivery to Multicellular Spheroids Tumour Models. *Biomaterials* **2011**, *32* (11), 2953–2958.

(28) Khormaee, S.; Choi, Y.; Shen, M. J.; Xu, B.; Wu, H.; Griffiths, G. L.; Chen, R.; Slater, N. K. H.; Park, J. K. Endosomolytic Anionic Polymer for the Cytoplasmic Delivery of SiRNAs in Localized in Vivo Applications. *Adv. Funct. Mater.* **2013**, *23* (5), 565–574.

(29) Liechty, W. B.; Chen, R.; Farzaneh, F.; Tavassoli, M.; Slater, N. K. H. Synthetic pH-Responsive Polymers for Protein Transduction. *Adv. Mater.* **2009**, *21* (38–39), 3910–3914.

(30) Lynch, A. L.; Chen, R.; Slater, N. K. H. pH-Responsive Polymers for Trehalose Loading and Desiccation Protection of Human Red Blood Cells. *Biomaterials* **2011**, *32* (19), 4443–4449.

(31) Chen, S.; Wang, S.; Kopytynski, M.; Bachelet, M.; Chen, R. Membrane-Anchoring, Comb-Like Pseudopeptides for Efficient, pH-Mediated Membrane Destabilization and Intracellular Delivery. *ACS Appl. Mater. Interfaces* **2017**, *9* (9), 8021–8029.

(32) Sowemimo-Coker, S. O. Red Blood Cell Hemolysis during Processing. *Transfus. Med. Rev.* **2002**, *16* (1), 46–60.

(33) Lynch, A. L.; Slater, N. K. H. Influence of Intracellular Trehalose Concentration and Pre-Freeze Cell Volume on the Cryosurvival of Rapidly Frozen Human Erythrocytes. *Cryobiology* **2011**, *63* (1), 26–31.

(34) Alotaibi, N. A. S.; Slater, N. K. H.; Rahmoune, H. Salidroside as a Novel Protective Agent to Improve Red Blood Cell Cryopreservation. *PLoS One* **2016**, *11* (9), e0162748.

(35) Thomas, J. L.; Borden, K. A.; Tirrell, D. A. Modulation of Mobilities of Fluorescent Membrane Probes by Adsorption of a Hydrophobic Polyelectrolyte. *Macromolecules* **1996**,

29 (7), 2570–2576.

(36) Polozova, A.; Winnik, F. M. Mechanism of the Interaction of Hydrophobically-Modified Poly-(*N*-Isopropylacrylamides) with Liposomes. *Biochim. Biophys. Acta - Biomembr.* **1997**, *1326* (2), 213–224.

(37) Resh, M. D. Fatty Acylation of Proteins: The Long and the Short of It. *Prog. Lipid Res.* **2016**, *63*, 120–131.

(38) Murthy, N.; Robichaud, J. R.; Tirrell, D. A.; Stayton, P. S.; Hoffman, A. S. The Design and Synthesis of Polymers for Eukaryotic Membrane Disruption. *J. Control. Release* **1999**, *61* (1–2), 137–143.

(39) Chen, T.; Mcintosh, D.; He, Y.; Kim, J.; Tirrell, D. A.; Scherrer, P.; Fenske, D. B.; Sandhu, A. P.; Cullis, P. R. Alkylated Derivatives of Poly (Ethylacrylic Acid) Can Be Inserted into Preformed Liposomes and Trigger pH-Dependent Intracellular Delivery of Liposomal Contents. *Mol. Membr. Biol.* **2004**, *21* (6), 385–393.

(40) Eroglu, A.; Toner, M.; Toth, T. L. Beneficial Effect of Microinjected Trehalose on the Cryosurvival of Human Oocytes. *Fertil. Steril.* **2002**, *77* (1), 152–158.

(41) Thomas, J. L.; Barton, S. W.; Tirrell, D. A. Membrane Solubilization by a Hydrophobic Polyelectrolyte: Surface Activity and Membrane Binding. *Biophys. J.* **1994**, *67* (3), 1101–1106.

(42) Krauson, A. J.; He, J.; Wimley, W. C. Determining the Mechanism of Membrane Permeabilizing Peptides: Identification of Potent, Equilibrium Pore-Formers. *Biochim.*

Biophys. Acta - Biomembr. **2012**, *1818* (7), 1625–1632.

(43) Guha, S.; Ghimire, J.; Wu, E.; Wimley, W. C. Mechanistic Landscape of Membrane-Permeabilizing Peptides. *Chem. Rev.* **2019**, *119* (9), 6040–6085.

(44) Hazel, J. R. Thermal Adaptation in Biological Membranes: Is Homeoviscous Adaptation the Explanation? *Annu. Rev. Physiol.* **1995**, *57* (1), 19–42.

(45) Satpathy, G. R.; Torok, Z.; Balia, R.; Dwyre, D. M.; Little, E.; Walker, N. J.; Tablina, F.; Crowe, J. H.; Tsvetkova, N. M. Loading Red Blood Cells with Trehalose: A Step towards Biostabilization. *Cryobiology* **2004**, *49* (2), 123–136.

(46) Gershfeld, N. L.; Murayama, M. Thermal Instability of Red Blood Cell Membrane Bilayers: Temperature Dependence of Hemolysis. *J. Membr. Biol.* **1988**, *101* (1), 67–72.

(47) Kopytynski, M.; Chen, S.; Legg, S.; Minter, R.; Chen, R. A Versatile Polymer-Based Platform for Intracellular Delivery of Macromolecules. *Adv. Therap.* **2020**, *3*, 1900169.

(48) Liu, F. F.; Dong, X. Y.; Sun, Y. Molecular Mechanism for the Effects of Trehalose on β-Hairpin Folding Revealed by Molecular Dynamics Simulation. *J. Mol. Graph. Model.* **2008**, *27* (4), 421–429.

(49) Zimmerberg, J.; Kozlov, M. M. How Proteins Produce Cellular Membrane Curvature. *Nat. Rev. Mol. Cell Biol.* **2006**, *7* (1), 9–19.

(50) Campelo, F.; McMahon, H. T.; Kozlov, M. M. The Hydrophobic Insertion Mechanism of Membrane Curvature Generation by Proteins. *Biophys. J.* **2008**, *95* (5), 2325–2339.

(51) Großauer, J.; Kosol, S.; Schrank, E.; Zangger, K. The Peptide Hormone Ghrelin Binds to Membrane-Mimetics via Its Octanoyl Chain and an Adjacent Phenylalanine. *Bioorg*. *Med*. *Chem*. **2010**, *18* (15), 5483–5488.

(52) McMahon, H. T.; Kozlov, M. M.; Martens, S. Membrane Curvature in Synaptic Vesicle Fusion and Beyond. *Cell* **2010**, *140* (5), 601–605.

(53) Iversen, L.; Mathiasen, S.; Larsen, J. B.; Stamou, D. Membrane Curvature Bends the Laws of Physics and Chemistry. *Nat*. *Chem*. *Biol*. **2015**, *11* (11), 822–825.

(54) Johnson, R. M. Membrane Stress Increases Cation Permeability in Red Cells. *Biophys*. *J*. **1994**, *67* (5), 1876–1881.

(55) Zweytick, D.; Tumer, S.; Blondelle, S. E.; Lohner, K. Membrane Curvature Stress and Antibacterial Activity of Lactoferricin Derivatives. *Biochem*. *Biophys*. *Res*. *Commun*. **2008**, *369* (2), 395–400.

(56) Chao, H.; Davies, P. L.; Carpenter, J. F. Effects of Antifreeze Proteins on Red Blood Cell Survival during Cryopreservation. *J*. *Exp*. *Biol*. **1996**, *199* (9), 2071–2076.

(57) Acker, J. The Use of Intracellular Protectants in Cell Biopreservation. In *Advances in Biopreservation*; Baust, J. G., Ed.; Taylor and Francis: New York, 2006; 299–320.

(58) Pallotta, V.; D'Amici, G. M.; D'Alessandro, A.; Rossetti, R.; Zolla, L. Red Blood Cell Processing for Cryopreservation: From Fresh Blood to Deglycerolization. *Blood Cells, Mol*. *Dis*. **2012**, *48* (4), 226–232.

Table of Contents Graphic